frontiers in Neuroscience

ORIGINAL RESEARCH
published: 08 March 2019
doi: 10.3389/fnins.2019.00201

Cell Autonomous Neuroprotection by the Mitochondrial Uncoupling Protein 2 in a Mouse Model of Glaucoma

*Daniel T. Hass and Colin J. Barnstable**

Department of Neural and Behavioral Sciences, College of Medicine, The Pennsylvania State University, Hershey, PA, United States

OPEN ACCESS

Edited by:
Peter Koulen, University of Missouri System, United States

Reviewed by:
Raghu Krishnamoorthy, University of North Texas Health Science Center, United States
Rafael Linden, Federal University of Rio de Janeiro, Brazil

***Correspondence:**
Colin J. Barnstable
cbarnstable@psu.edu;
cbarnstable@pennstatehealth.psu.edu

Specialty section:
This article was submitted to Neurodegeneration, a section of the journal Frontiers in Neuroscience

Received: *10 January 2019*
Accepted: *20 February 2019*
Published: *08 March 2019*

Citation:
Hass DT and Barnstable CJ (2019) Cell Autonomous Neuroprotection by the Mitochondrial Uncoupling Protein 2 in a Mouse Model of Glaucoma. Front. Neurosci. 13:201. doi: 10.3389/fnins.2019.00201

Glaucoma is a group of disorders associated with retinal ganglion cell (RGC) degeneration and death. There is a clear contribution of mitochondrial dysfunction and oxidative stress toward glaucomatous RGC death. Mitochondrial uncoupling protein 2 (*Ucp2*) is a well-known regulator of oxidative stress that increases cell survival in acute models of oxidative damage. The impact of *Ucp2* on cell survival during sub-acute and chronic neurodegenerative conditions, however, is not yet clear. Herein, we test the hypothesis that increased *Ucp2* expression will improve RGC survival in a mouse model of glaucoma. We show that increasing RGC but not glial *Ucp2* expression in transgenic animals decreases glaucomatous RGC death, but also that the PPAR-γ agonist rosiglitazone (RSG), an endogenous transcriptional activator of *Ucp2*, does not significantly alter RGC loss during glaucoma. Together, these data support a model whereby increased *Ucp2* expression mediates neuroprotection during a long-term oxidative stressor, but that transcriptional activation alone is insufficient to elicit a neuroprotective effect, motivating further research in to the post-transcriptional regulation of *Ucp2*.

Keywords: retina, RGC, Ucp2, glaucoma, neuroprotection, mitochondria, oxidative stress

INTRODUCTION

Glaucoma is a group of disorders associated with retinal ganglion cell (RGC) degeneration and death (Quigley, 2011) and, after cataracts, is the most frequent cause of blindness worldwide (Resnikoff and Keys, 2012). An increase in intra-ocular pressure (IOP) is a prominent risk factor for glaucoma (Boland and Quigley, 2007), and most therapeutic solutions designed to prevent RGC death in glaucoma share the ability to decrease IOP. However, IOP reduction does not reduce glaucomatous visual field loss in roughly half of patients (Leske et al., 2004), necessitating development of adjuvant therapeutic modalities, including neuroprotective molecules that can protect RGCs.

The molecular mechanisms of glaucoma pathogenesis are multifactorial, but are frequently connected to an increase in damaging free radicals in the eye (Izzotti et al., 2003; Saccà and Izzotti, 2008), retina (Tezel et al., 2005), and optic nerve head (Malone and Hernandez, 2007; Feilchenfeld et al., 2008), herein termed oxidative stress. Ocular hypertension increases RGC oxidative stress (Chidlow et al., 2017), despite anti-oxidative support from endogenous antioxidant proteins (Munemasa et al., 2009) and resident glial cells of the retina, including astrocytes and müller glia (Varela and Hernandez, 1997; Carter-Dawson et al., 1998; Kawasaki et al., 2000; Woldemussie et al., 2004). Exogenous addition of serum antioxidants such as vitamin E is not necessarily protective from the disease (Ramdas et al., 2018), suggesting that current anti-oxidative therapeutics for glaucoma are insufficient. The early transcriptional responses of DBA2/J mouse RGCs to elevated IOP strongly suggest mitochondrial abnormalities in RGCs early in the disease (Williams et al., 2017), which appears to persist in multiple animal models (Coughlin et al., 2015; Takihara et al., 2015; Ito and Di Polo, 2017) as well as in human glaucoma (Abu-Amero et al., 2006; Piotrowska-Nowak et al., 2018).

Mitochondria are a well-known source of cellular free radicals, which during oxidative phosphorylation can leak from multi-protein complexes of the electron transport chain such as NADH:Ubiquinone Oxidoreductase and Coenzyme Q:Cytochrome C Oxidoreductase (St-Pierre et al., 2002). Mitochondrial ROS production is greater at hyperpolarized mitochondrial membrane potentials (Ψ_m), and in isolated mitochondria small decreases in Ψ_m significantly decrease levels of ROS (Korshunov et al., 1997; Miwa et al., 2003). Endogenous uncoupling proteins, particularly the mitochondrial uncoupling protein 2 (UCP2), are able to protect nervous tissue from multiple sources of acute damage (Mattiasson et al., 2003; Andrews et al., 2005; Lapp et al., 2014; Barnstable et al., 2016) by decreasing Ψ_m and presumably ROS (Fleury et al., 1997; Echtay et al., 2001). Lower levels of ROS are protective in most scenarios, but the predicted outcome of a lower Ψ_m is also a decreased mitochondrial drive for ATP synthesis (Klingenberg and Rottenberg, 1977). Therefore, it is unclear whether uncoupling proteins are beneficial for long-term neurodegenerative conditions. As with many neurodegenerative disorders, the clinical course of glaucoma progresses over multiple years. It is therefore essential that model systems of neurodegeneration develop over time and not in reaction to a single damaging insult.

In the microbead model of glaucoma, occlusion of the irido-corneal angle progressively increases damage to RGCs over a sub-acute time frame (Huang et al., 2018). Using this model, we tested whether enhanced *Ucp2* expression in mouse RGCs or in supporting glial cells is protective against injury. We found that increasing levels of *Ucp2* in RGCs, but not in GFAP-expressing glia, were neuroprotective. *Ucp2* levels are under several forms of transcriptional and translational control (Donadelli et al., 2014; Lapp et al., 2014), and our second goal was to determine whether factors that increase *Ucp2* transcription provide protection from cell death. We found that the PPAR-γ agonist rosiglitazone (RSG), a well-known transcriptional activator of Ucp2, does not alter RGC survival during glaucoma, implying an additional need to characterize clinically useful molecules which regulate *Ucp2* at post-transcriptional levels.

MATERIALS AND METHODS

Ethics Statement

This study was carried out in accordance with the National Research Council's Guide for the Care and Use of Laboratory Animals (8th edition). The protocol was approved by the Pennsylvania State University College of Medicine Institutional Animal Care and Use Committee.

Animals

Wild-type (WT) C57BL6/J and transgenic mice were housed in a room with an ambient temperature of 25°C, 30–70% humidity, a 12-h light–dark cycle, and *ad libitum* access to rodent chow. Transgenic mouse strains, B6.Cg-Tg(*GFAP-cre/ER^{T2}*)505Fmv/J (*Gfap-creER^{T2}*, Stock#: 012849) (Ganat et al., 2006) and Tg(*Thy1-cre/ER^{T2}*,-EYFP)HGfng/PyngJ *(Thy1-creER^{T2}*, Stock#: 012708) (Young et al., 2008), were each generated on a WT background and purchased from the Jackson Laboratory (Bar Harbor, ME, United States). *GFAP-creER^{T2}* and *Thy1-creER^{T2}* mice express a fusion product of *cre* recombinase and an estrogen receptor regulatory subunit (*creER^{T2}*) under the control of the *hGFAP* or *Thy1* promoters, respectively. CreER^{T2} activity is regulated by the estrogen receptor modulator and tamoxifen metabolite 4-hydroxytamoxifen (Zhang et al., 1996). Ucp2KI$^{fl/fl}$ mice were derived from Ucp2KOKI$^{fl/fl}$ mice (provided by Sabrina Diano, Ph.D.) and result from multiple back-crosses with WT mice (Toda et al., 2016). In these crosses, mice were selectively bred to retain the Ucp2KI sequence and the WT variant of the *Ucp2* gene. In these mice, a transgene was inserted in to the R26 locus, containing a LoxP-flanked stop codon followed by a copy of the mouse *Ucp2* cDNA and an IRES-EGFP sequence. Following cell-type specific cre-mediated excision of the LoxP-flanked stop codon, these mice express *Ucp2* and EGFP in astrocytes and müller glia (*Ucp2^{KI}; GFAP-creER^{T2}* mice) or in the vast majority of RGCs (*Ucp2^{KI}; Thy1-creER^{T2}* mice*)*. To elicit cre-mediated excision of this stop codon, we injected mice intraperitoneally with 100 mg tamoxifen (Sigma, T5648)/kg mouse/day for 8 days, preceding any experimental manipulations. Same-litter cre recombinase-negative control mice (*Ucp2^{KI}*) were also injected with tamoxifen to control for any potential biological impacts of tamoxifen.

Rosiglitazone was fed to WT mice by grinding 4 mg pills (Avandia, GSK) with a mortar and pestle and mixing them into ground normal mouse chow. We measured daily food consumption and adjusted the amount of RSG used based on food consumption. RSG was fed to mice beginning 2 days prior to microbead injection and does not alter IOP. During this study, we estimate an average RSG consumption of 28.2 mg RSG/kg mouse/day.

Microbead Injection

We modeled glaucoma in mice by elevating IOP. We increased IOP in 2–4 month old mice of both genders as previously described (Cone et al., 2012). At least 24 h prior to bead injection, we took a baseline IOP measurement. Prior to bead injection, IOP is stable and is well represented by a single measurement. Immediately prior to bead injection, we anesthetized mouse corneas topically with proparacaine hydrochloride (0.5%) eyedrops and systemically with an intraperitoneal injection of 100 mg/kg ketamine/10 mg/kg xylazine. While anesthetized, we injected 6 μm (2 μL at 3×10^6 beads/μL; Polysciences, Cat#: 07312-5) and 1 μm (2 μL at 1.5×10^7 beads/μL; Polysciences, Cat#: 07310-15) polystyrene microbeads through a 50–100 μm cannula in the cornea formed by a beveled glass micropipette connected by polyethylene tubing to a Hamilton syringe (Hamilton Company Reno, NV, United States). As an internal control, 4 μL of sterile 1× phosphate buffered saline (PBS) was injected in to the contralateral eye. We measured postoperative IOP every 3 days for 30 days. Following terminal IOP measurements, mice were asphyxiated using a Euthanex SmartBox system, which automatically controls CO_2 dispersion, followed by cervical dislocation.

IOP Measurement

Intra-ocular pressure was measured in mice anesthetized by 1.5% isoflurane in air (v/v) using an Icare® TonoLab (Icare Finland Oy, Espoo, Finland) rebound tonometer, both before and after injection with polystyrene microbeads. Each reported measurement is the average of 18 technical replicates/mouse/eye. Mice were included in this study if their individual IOP was elevated by ≥3 mmHg or if a paired *t*-test of IOP over time between microbead and PBS-injected eyes was statistically significant ($p < 0.05$). Baseline and bead-injected IOPs were compared between mouse strains to confirm the absence of any genotype-dependent differences in IOP increase.

Histology and Immunocytochemistry

Immunolabeling of sectioned retinal tissue was performed as previously described (Pinzon-Guzman et al., 2011). Briefly, whole eyes were fixed in 4% paraformaldehyde (Electron Microscopy Sciences, Hatfield, PA, United States) in 1× PBS overnight at 4°C. The next day, eyes were divided in half with a scalpel blade. One half was frozen and sectioned, while the other was labeled as a whole-mount. Frozen tissues were embedded in a 2:1 mixture of 20% sucrose and OCT (Electron Microscopy Sciences), cooled to −20°C, and cut at a 10 μm thickness. Samples for each experiment were located on the same slide to control for assay variability. Prior to immunohistochemical labeling, we unmasked antigens by exposing them to a 10 mM sodium citrate buffer (pH6.0) for 30 min at 100°C. Subsequent labeling of oxidative protein carbonyls was performed using an OxyIHC kit (EMD-Millipore, Cat#: S7450). Derivatization of protein carbonyl groups and all subsequent steps were performed in accordance with the manufacturer's instructions. Staining intensity was derived using the H-DAB vector of the ImageJ Color Deconvolution tool background was subtracted from each image, resulting in a numerical semiquantitative measure of oxidative tissue stress. Tissue was imaged using an Olympus BX50 microscope. In this and all other experiments, the acquisition parameters for any given label were held constant.

Post-fixation, retinal whole mounts were permeabilized with 0.2% Triton-X-100 in PBS, blocked with 5% non-fat milk, and incubated in rabbit anti-RBPMS antibody (1:500, EMD Millipore) for 6 days at 4°C. Tissue was incubated in secondary antibody and 1 μg/mL Hochest-33258 overnight at 4°C prion to washing and mounting with 0.5% n-propyl gallate in 1:1 glycerol: PBS. Whole-mount tissue was imaged on a Fluoview FV1000 confocal microscope (Olympus).

Retinal Ganglion Cell Counting

Retinal ganglion cells were counted in retinal whole-mounts using the marker RBPMS (Rodriguez et al., 2014) across three to four 317.95 μm × 317.95 μm fields, with each field centered 1000 μm from the optic nerve head. Cell counts were converted to measurements of RGC density, averaged for a single retina, and RGC survival was calculated as a percentage of bead-injected RGC density over contralateral control PBS-injected RGC density. RGC loss or death was 100-mean RGC survival for a given sample. The counter was blinded to the identity of each sample. We did not find a significant effect of retinal quadrant on RGC density normally or with elevated IOP, and our images were therefore taken across all retinal quadrants. The mean±SEM and median $RBPMS^+$ RGC densities in PBS-injected retinas (pooled from WT C57BL6/J and $Ucp2^{KI}$ controls) were 4758±113 and 4738 cells/mm^2, respectively. The mean±SEM and median $RBPMS^+$ RGC densities in bead-injected retinas were 3957±152 and 3858 cells/mm^2, respectively, leading to an average 17% cell loss 30 days following bead injection.

RNA Isolation and Quantitative Real-Time PCR

Flash frozen cells or tissue were lyzed in TRIzol (Thermo-Fischer, Cat#:15596018) and RNA precipitated using the manufacturer's recommended procedure. Final RNA concentration was measured using a NanoDrop ND-1000 Spectrophotometer prior to reverse transcription. We reverse transcribed 300–1000 μg RNA using SuperScript III (Thermo-Fischer, Cat#: 18080093) with random hexamers. cDNA was amplified with iQ SYBR Green Supermix (Bio-Rad, Cat#: 1708882) and amplified on a Bio-Rad iCycler. *Ucp2* primer sequences were F: 5′—GCT CAG AGC ATG CAG GCA TCG—3′ and R: 5′—CGT GCA ATG GTC TTG TAG GCT TCG—3′. TATA-box binding protein (*Tbp)* primer sequences were F: 5′—ACC TTA TGC TCA GGG CTT GGC C—3 R: 5′—GTC CTG TGC CGT AAG GCA TCA TTG—3′. Cq′s from *Ucp2* amplification were normalized against *Tbp* and controls using the $\Delta\Delta C_t$ method. Expression of *Ucp2/Tbp* in DBA2J retinas was analyzed from data deposited in the NCBI Gene Expression Omnibus (Geo) by Howell et al. (2011), under the accession GSE26299.

Primary Astrocyte Culture

Primary mouse cortical astrocytes were isolated from postnatal day 1–4 mice as previously described (Sarafian et al., 2010;

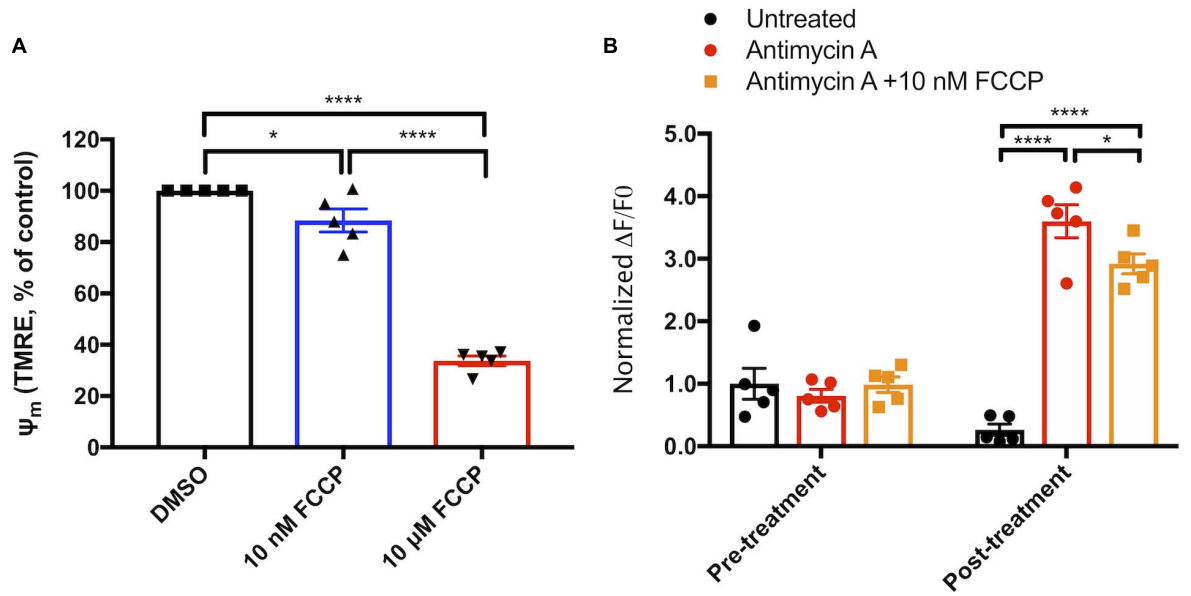

FIGURE 1 | Mitochondrial uncoupling decreases reactive oxygen species production. **(A)** Measurements of TMRE fluorescence as a proxy for mitochondrial membrane potential (Ψ_m) in cells exposed to vehicle, 10 nM FCCP, or 10 μM FCCP ($n = 3$). **(B)** Increase in MitoSox oxidation over a 5-min period prior to and following exposure of primary cortical astrocytes to nothing (black circles), 5 μM antimycin A (red circles), or 5 μM antimycin A and 10 nM FCCP (orange circles, $n = 5$). $^*p < 0.05$, $^{****}p < 0.0001$.

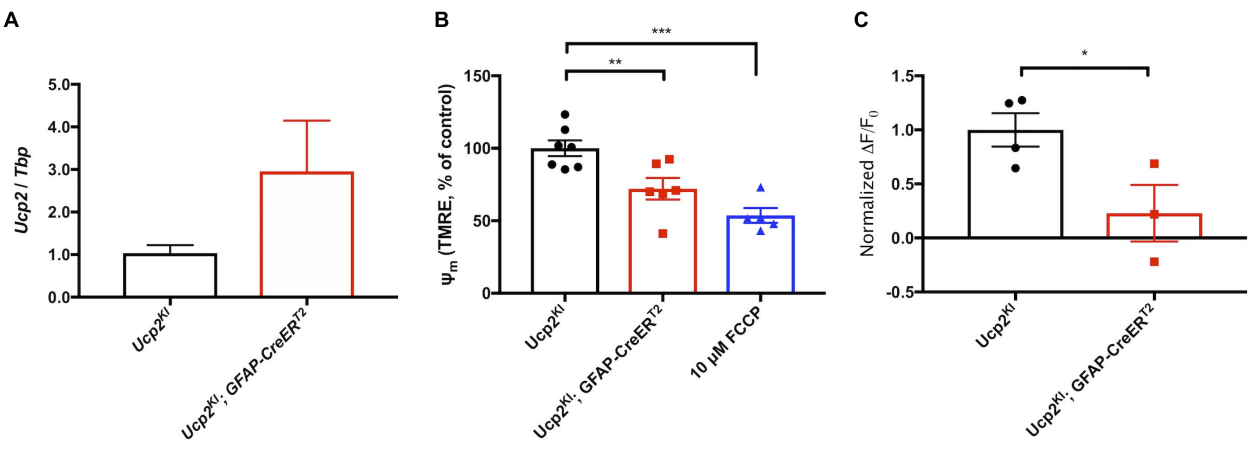

FIGURE 2 | Ucp2 decreases Ψ_m, increasing respiration and decreasing production of ROS. **(A)** Ucp2 gene expression ($n = 3$), **(B)** relative TMRE fluorescence (Ψ_m, $n = 5$–7), and **(C)** the relative rate of increase in MitoSox fluorescence ($n = 3$–4) within primary cortical astrocytes isolated from *Ucp2*^{KI} and *Ucp2*^{KI}*; Gfap-creER*^{T2} mice. $^*p < 0.05$, $^{**}p < 0.01$, $^{***}p < 0.005$.

Lapp et al., 2014). Briefly, mice were decapitated and brains were removed from the skull. In tissue culture medium, a ∼1 cm portion of superior cerebral cortex was pinched off of the brain using curved forceps. Meninges were removed, and the tissue was triturated with a sterile flame-polished glass Pasteur pipette until it formed a single cell suspension, approximately 20×. The suspension was filtered through a 70 μm cell strainer (Corning, Cat#: 352350) to remove larger debris, centrifuged at 500 × *g* and 4°C for 5 min, resuspended in growth medium (Dulbecco's Modified Eagle's Medium/Ham's F12 supplemented with 2 mM L-glutamine, 15 mM HEPES, 10% fetal bovine serum, and 10 ng/mL gentamicin), and plated in a T-25 tissue culture flask. Cells were grown at 37°C in a 5% CO_2/balance air atmosphere. After the cells reached confluence, between 7–14 days *in vitro* (DIV), contaminating cells were shaken off by rotating at 250 RPM overnight. Astrocyte-enriched cultures were plated at 30,000 cells/well on black tissue-culture-treated 96-well plates (Corning, Cat#3603) and used at passage #2 or 3, allowing at least 48 h following medium replacement before experimentation. All cells used in this study were exposed to 1 μM 4-hydroxytamoxifen (Sigma, Cat#: H6278) for 24 h prior to studies of *Ucp2* function.

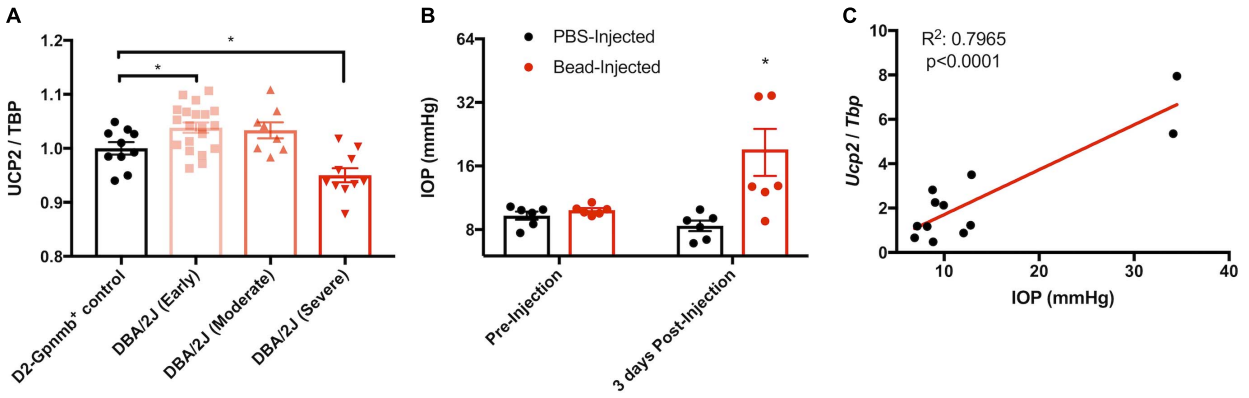

FIGURE 3 | Glaucoma increases *Ucp2* expression. **(A)** *Ucp2* expression in a genome-wide microarray of gene expression in the retinas of DBA/2J mice at various stages of glaucoma (n = 10–20), and DBA/2J-Gpnmb^{+} controls (n = 10; Howell et al., 2011). **(B)** Intra-ocular pressure (IOP) prior to and following microbead injection (n = 6) and **(C)** expression of *Ucp2* in each of the retinas from these mice as a function of IOP, 3 days following bead injection (n = 12). *$p < 0.05$.

Measurement of Mitochondrial Membrane Potential and Oxidative Status

We determined mitochondrial membrane potential (Ψ_m) and oxidative status of primary cortical astrocytes using the mitochondrial membrane potential-sensitive dye TMRE (50 nM, ImmunoChemistry, Cat#: 9103) or the mitochondrial superoxide probe MitoSox (5 μM, Thermo-Fischer, Cat#: M36008), which is selectively targeted to mitochondria. Cells were incubated in either dye in prewarmed assay medium (1× PBS supplemented with 1 mM glucose and 2 mM GlutaMax, Thermo-Fischer, Cat#: 35050-061) for 30 min at 37°C, followed by two washes and imaging. MitoSox fluorescence intensity was measured using the kinetic mode of a microplate reader (BioTek Synergy II), which took serial measurements of MitoSox fluorescence over time. The rate of increase in fluorescence (ΔF) over 10 min was divided by initial fluorescent intensity (F_0) for each well. This rate of increase was normalized to the mean $\Delta F/F_0$ of control cells. We verified the utility of TMRE as an indicator of Ψ_m by simultaneously treating cells with the membrane permeant protonophore carbonyl cyanide-*4*-(trifluoromethoxy) phenylhydrazone (FCCP, 10 μM, Caymen Chemical, Cat#: 15218), which depolarizes Ψ_m. Similarly, we used the mitochondrial complex III inhibitor antimycin A (AA, 5 μM) to stimulate ROS production and confirm the utility of MitoSox as an indicator of ROS.

Statistical Analysis

Quantified data are represented by that group's mean±SEM unless otherwise indicated. We performed all statistical analyses in GraphPad Prism. We determined the statistical effect of one independent variable (such as genetic background) on two groups using a Student's t-test or paired sample t-test in cases where samples were matched (e.g., the control was the contralateral eye of the same animal). We analyzed the effect of one variable on >2 groups (e.g., comparisons of *Ucp2*^{KI} with or without each *cre* variant) using a one-way ANOVA with a Bonferroni *post hoc* analysis. We analyzed the effect of two variables (e.g., the effects AA and FCCP on MitoSox) using a two-way ANOVA with a Bonferroni's *post hoc* analysis. The statistical significance threshold was set at $p < 0.05$ for all tests.

In ANOVAS of unmatched samples, Prism automatically implements a Geisser-Greenhouse correction to improve statistical analysis of non-spherical data sets. In accordance with the Prism Statistics guide, we assumed sphericity in matched data sets (i.e., in bead- vs. PBS-injected eyes, and cells treated with different groups of respiratory chain inhibitors).

RESULTS

Exogenous Uncoupling Agents Decrease the Generation of Mitochondrial ROS

The positive association between mitochondrial membrane potential (Ψ_m) and the production of reactive oxygen species (ROS) has been well characterized in isolated mitochondria, and we tested the hypothesis that mild mitochondrial uncoupling stimulated by an exogenous protonophore will decrease mitochondrial ROS in intact cells. We treated primary cortical astrocytes with FCCP at a low concentration to uncouple mitochondria without completely dissipating the Ψ_m, and found that 10 nM FCCP depolarized the mitochondrial membrane potential (Ψ_m) to 88±4% of control levels, whereas Ψ_m was 34±2% of control in astrocytes treated with 10 μM FCCP, a concentration routinely used to maximally depolarize mitochondria (10 μM; **Figure 1A**); 10 nM FCCP added to MitoSox loaded cells did not significantly alter mitochondrial superoxide generation (data not shown), so we tested the hypothesis that uncoupling will reduce ROS production by dysfunctional mitochondria. To test this hypothesis, we loaded cells with the mitochondrion-targeted superoxide probe MitoSox and treated them with the mitochondrial complex III inhibitor AA (5 μM). AA significantly increased the rate of MitoSox oxidation ($p < 0.001$,

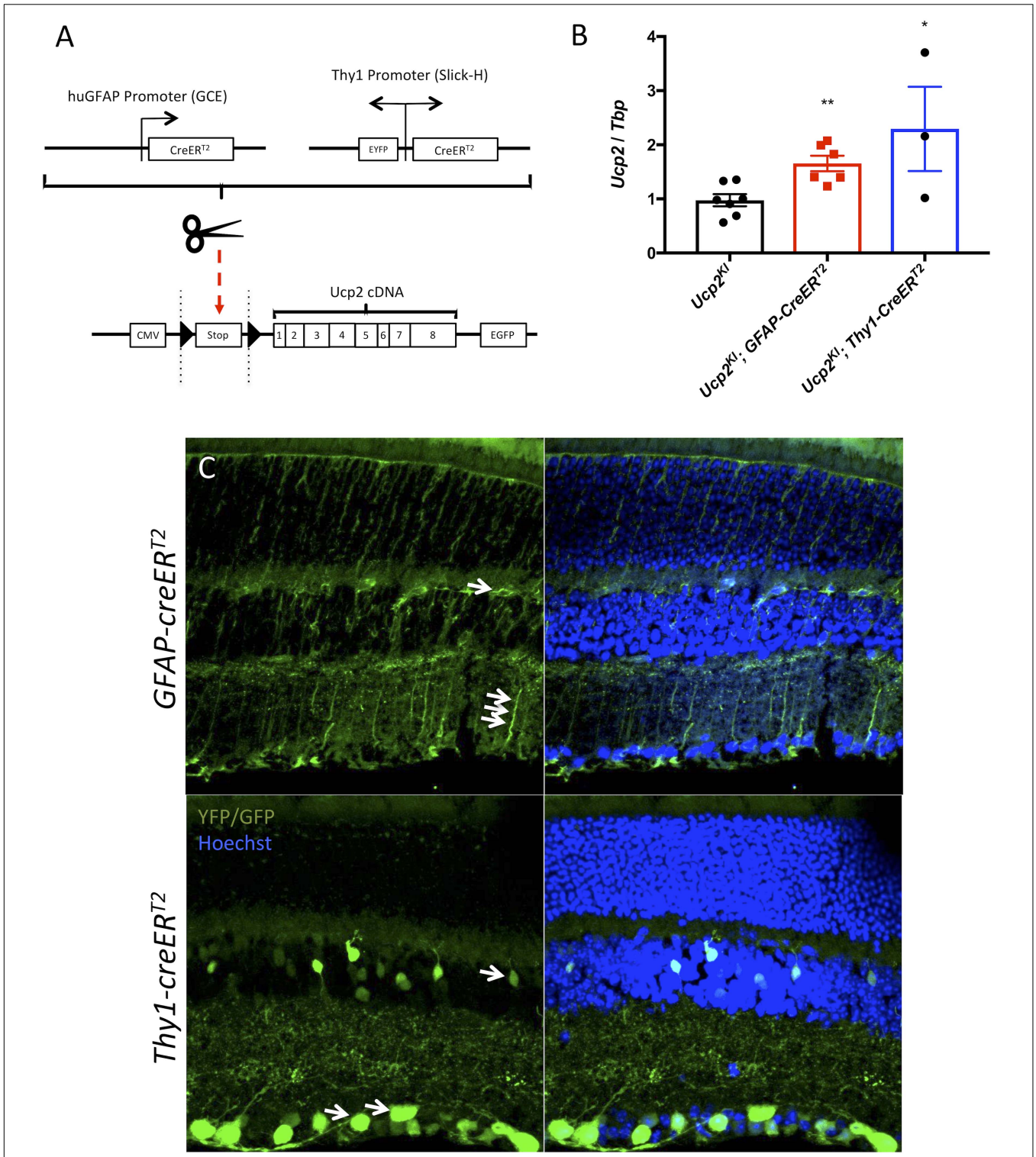

FIGURE 4 | Effects of *Thy1-creER*^{T2} and *Gfap-creER*^{T2} on retinal *Cre* recombinase localization and Ucp2 expression. **(A)** Gene diagram of transgenic *Ucp2* and *cre* recombinase variants used in the present study. **(B)** Expression of *Ucp2* in control and transgenic mice ($n = 3$). **(C)** Hoechst 33258 (blue)-labeled frozen sections of *Ucp2*^{KI}*; GFAP-creER*^{T2} and *Ucp2*^{KI}*; Thy1-creER*^{T2} retinas, showing the endogenous fluorescence of EGFP and YFP, respectively. White arrows point to Muller glia filaments and cell bodies in *GFAP-creER*^{T2} retinas and to RGC soma in *Thy1-creER*^{T2} retinas. *$p < 0.05$, **$p < 0.01$.

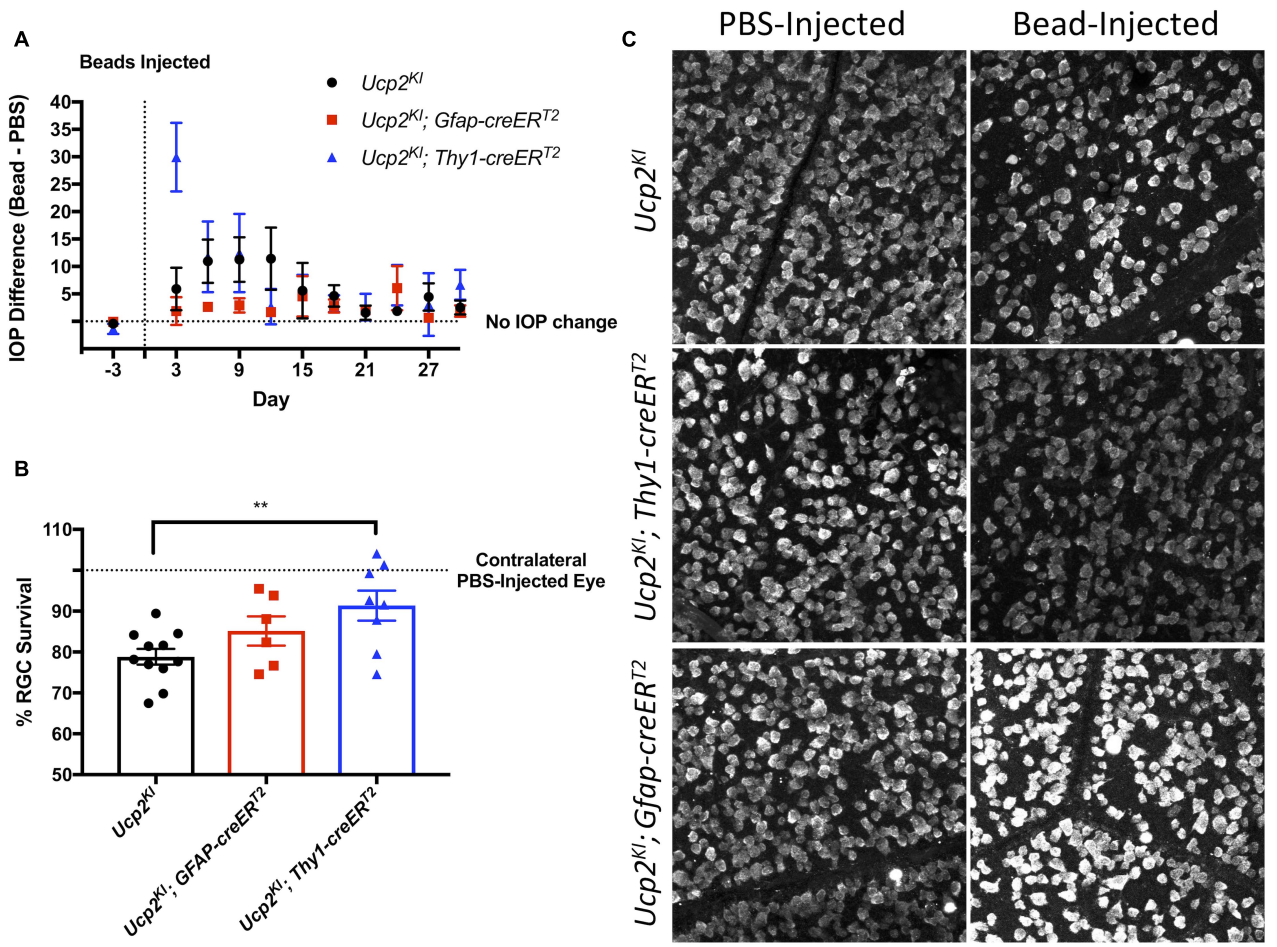

FIGURE 5 | Increased *Ucp2* expression in RGCs but not astrocytes and müller glia decreases retinal ganglion cell loss. **(A)** Difference IOP between bead- and PBS-injected eyes before and following intraocular surgery. Beads injection elevated IOP over a 30-day period in $Ucp2^{KI}$ ($n = 11$), $Ucp2^{KI}$; *Gfap-creER*^{T2} ($n = 6$), $Ucp2^{KI}$; *Thy1-creER*^{T2} ($n = 9$) eyes. **(B)** Percentage RGC survival in retinal whole-mounts from bead-injected eyes, relative to retinas of PBS-injected contralateral control eyes. **(C)** Representative images of retinal whole-mounts labeled for RBPMS, quantified in **B**. $^{**}p < 0.01$.

Figure 1B), but this increase was partially attenuated in cells simultaneously treated with AA and 10 nM FCCP ($p < 0.05$, **Figure 1B**). These data show that uncoupling decreases the generation of ROS by cultured astrocytes with dysfunctional mitochondria.

Uncoupling Protein 2 Decreases Ψ_m and ROS Production

To determine whether mitochondrial uncoupling proteins have the same cellular effects as chemical protonophores on Ψ_m and ROS production, we isolated cortical astrocytes from $Ucp2^{KI}$; *GFAP-creER*^{T2} mice. *Ucp2* expression is elevated roughly threefold in *GFAP-creER*^{T2} expressing cells of these mice following exposure to 4-hydroxytamoxifen (**Figure 2A**), and we tested the hypothesis that the addition of transgenic *Ucp2* will decrease Ψ_m and the generation of ROS. Our data show that Ucp2 knock-in depolarizes Ψ_m to 72±7% of control levels ($p = 0.0095$, **Figure 2B**), with 10 μM FCCP decreasing TMRE fluorescence to 54±5% of controls ($p = 0.0002$). Increasing Ucp2 levels decreased the production of ROS, monitored by the change in MitoSox fluorescence over time and normalized to the mean fluorescent intensity of $Ucp2^{KI}$ control samples ($p = 0.043$; **Figure 2C**). Together, these data show that increased Ucp2 expression decreases Ψ_m and mitochondrial ROS, which may be similar in mechanism to the protective effects promoted by 10 nM FCCP.

Elevated IOP Increases Ucp2 Expression

To determine whether Ucp2 expression is positively or negatively related to the progression of glaucoma, we analyzed publically available data from a microarray that determined gene expression changes in the retina and optic nerve heads of 10.5 month old DBA/2J mice and DBA/2J; $Gpnmb^{+}$ controls (Howell et al., 2014). DBA/2J are genetically predisposed toward glaucoma, and DBA/2J; $Gpnmb^{+}$ controls are genetically identical to these mice, except for in the *Gpnmb* gene, for which these control mice express a WT copy. Relative to the housekeeping gene *Tbp*, *Ucp2* expression is elevated

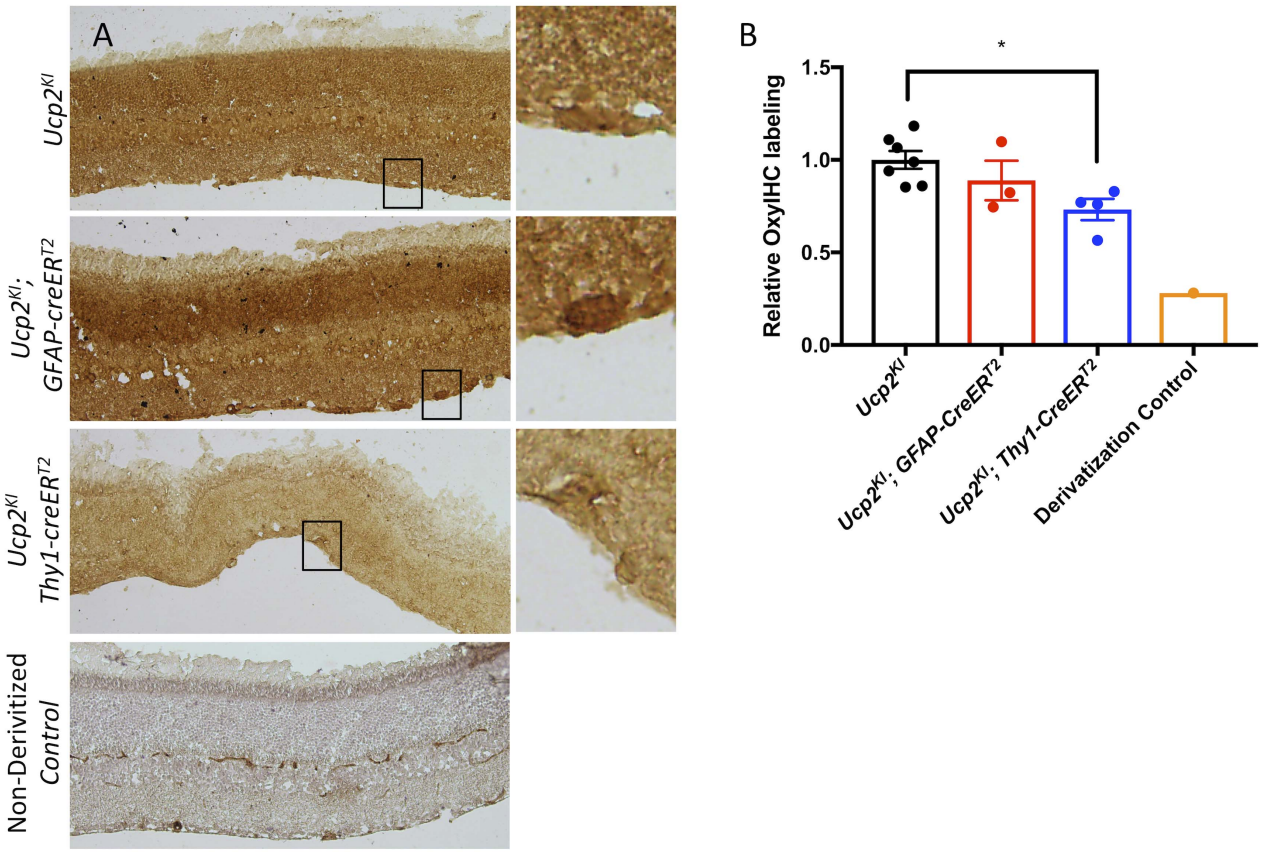

FIGURE 6 | Increased *Ucp2* expression in RGCs but not astrocytes and müller glia decreases oxidative stress. **(A)** Representative labeling of fixed retinas from bead-injected *Ucp2*^{KI} (n = 7), *Ucp2*^{KI}*; Gfap-creER*^{T2} (n = 3), and *Ucp2*^{KI}*; Thy1-creER*^{T2} (n = 4) eyes for oxidative stress-derived protein carbonylation. A single section was labeled without using the 2′,4′-dinitrophenylhydrazine derivitization reagent to confirm the specificity of the primary antibody to toward dinitrophenylhydrazones. **(B)** The intensity of DAB labeling is quantified. *$p < 0.05$.

early in glaucoma, but decreases with increasing disease severity ($p < 0.05$, **Figure 3A**). We confirmed these data in a microbead model of glaucoma, and found that 3 days following microbead injection, IOP is significantly elevated ($p < 0.05$, **Figure 3B**). Following IOP measurement, we determined Ucp2 expression in the retinas of these mice, and found that Ucp2 expression increases proportionally with IOP (r^2=0.8, p = 0.0001 **Figure 3C**). These data suggest that Ucp2 may play a role in the retinal response to IOP elevation.

Elevated Ucp2 Expression in RGCs but Not Astrocytes or Müller Glia Is Protective Against Glaucoma

To determine whether the protective effects of *Ucp2* expression in cells translate to the same *in vivo* system, we used mice in which Ucp2 expression can be increased in *Gfap*- or *Thy1*-expressing cells following exposure to tamoxifen (**Figure 4A**). Following eight consecutive 100 mg/kg/day injections, we found that *GFAP-creER*^{T2} expression increased *Ucp2* transcript levels to 165±14% of control ($p < 0.01$, n = 6), and *Thy1-creER*^{T2} increased Ucp2 to 229±77% of *Ucp2*^{KI} controls ($p < 0.05$, n = 3, **Figure 4B**).

Although *Thy1-creER*^{T2} retinas express YFP both before and following exposure to tamoxifen, *GFAP-creER*^{T2} retinas only express eGFP following LoxP excision. We show that eGFP and YFP are present in the retina, with localizations consistent with Gfap-expressing glia and RGCs, respectively, for the *GFAP-creER*^{T2} and *Thy1-creER*^{T2} transgenes (**Figure 4C**). The white arrows indicate regions of endogenous fluorophore expression, corresponding to müller glia cell bodies and fibers (top image), as well as RGC soma (bottom image) (**Figure 4C**). Notably, *Thy1-creER*^{T2} expression was not limited to the ganglion cell layer, implying cre activity in some inner nuclear layer cells.

We injected microbeads or PBS in to the anterior chambers of these mice, elevating IOP by an average of 5.3 mmHg in *Ucp2*^{KI} control mice (n = 11), 2.4 mmHg in *Ucp2*^{KI}; *GFAP-creER*^{T2} mice (n = 6), and 7.5 mmHg in *Ucp2*^{KI}; *Thy1-creER*^{T2} mice (n = 9, **Figure 5A**). Bead injection in control mice caused a significant loss in RGCs (A 19±3% reduction in RGC density) that was attenuated in mice overexpressing Ucp2 in RGCs (*Ucp2*^{KI}; *Thy1-creER*^{T2}, a 10±4% reduction), but not in *Ucp2*^{KI}; *GFAP-creER*^{T2} mice (a 15±4% reduction,

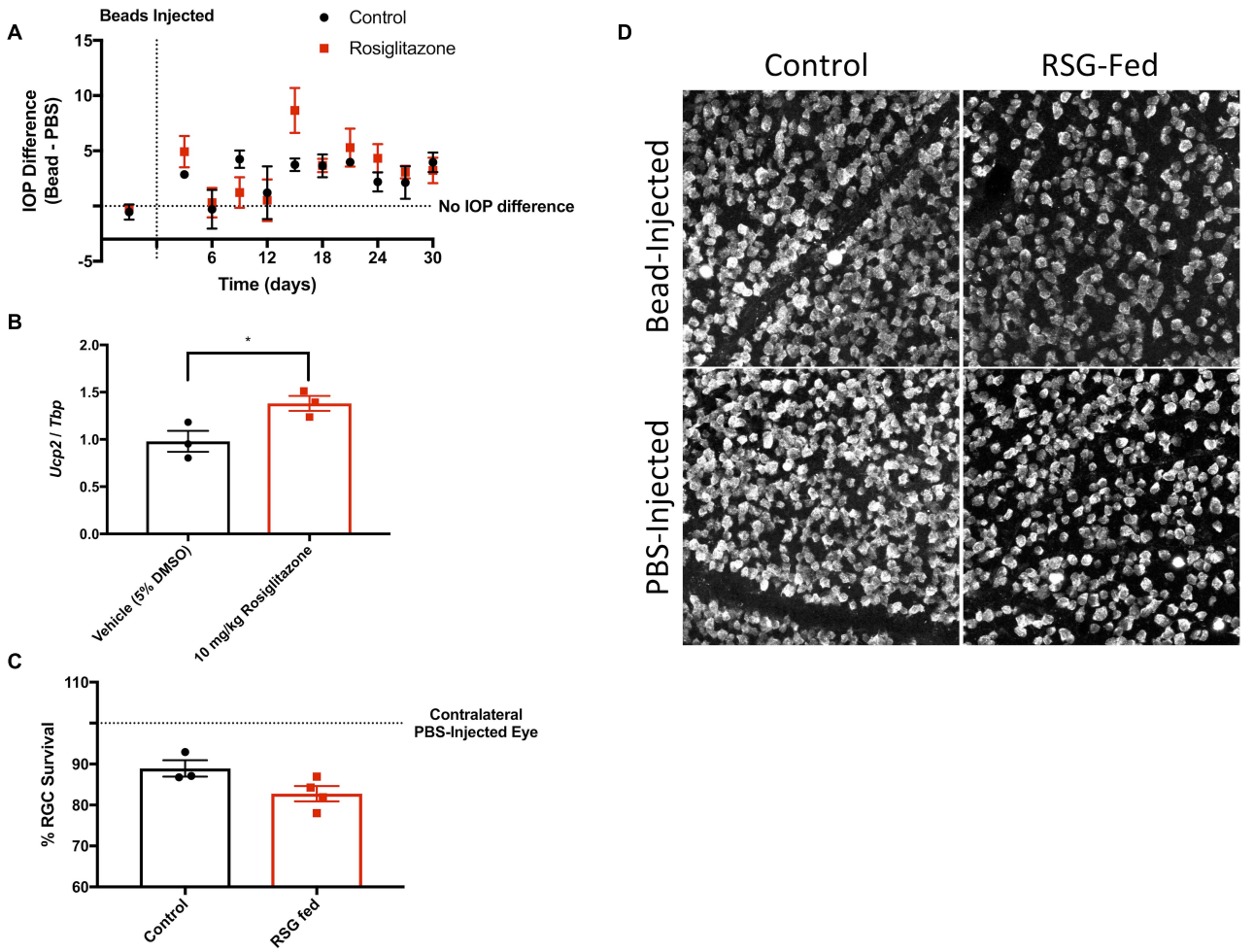

FIGURE 7 | Rosiglitazone increases *Ucp2* transcription but does not alter glaucomatous RGC loss. **(A)** Microbead injection increases IOP to a similar extent in control- and rosiglitazone (RSG)-fed mice. **(B)** Intraperitoneal RSG increases Ucp2 transcript levels in the mouse retina. **(C)** Increased IOP leads to RGC loss (decreased % survival), though dietary RSG does not appear to alter RGC loss. **(D)** Representative RBPMS labeling in whole-mount retinas from PBS- and bead-injected C57BL6J mice. $^*p < 0.05$.

Figures 5C,D). These data demonstrate that Ucp2 decreases RGC loss due to elevated IOP over a sub-acute timeframe, and also that the beneficial effects of Ucp2 are cell autonomous, as Ucp2-overexpression in *GFAP*-positive glia is insufficient to decrease glaucoma-related RGC loss (**Figure 5C**). The protective effects of Ucp2 expression coincided with significant decreases in oxidative protein carbonylation, measured by OxyIHC labeling. Bead-injected retinas from $Ucp2^{KI}$; $Thy1\text{-}creER^{T2}$ mice ($n = 4$) were labeled 27±6% less strongly than corresponding $Ucp2^{KI}$ controls ($p < 0.05$, $n = 7$). In contrast, labeling of $Ucp2^{KI}$; $GFAP\text{-}creER^{T2}$ retinas was non-significantly reduced by 11±11% ($n = 3$, **Figures 6A,B**) relative to controls.

Transcriptional Activation of Ucp2 Is Insufficient to Decrease Microbead-Induced RGC Loss

Past literature suggests that Ucp2 transcription is in part regulated by a PGC1-α/PPAR-γ axis (Chen et al., 2006; Donadelli et al., 2014). RSG is an FDA-approved PPAR-γ agonist. We confirmed that retinal *Ucp2* expression can increase 24 h following exposure to 10 mg/kg RSG (**Figure 7B**), and hypothesized that due to transcriptional activation of Ucp2, dietary RSG confers the same resistance to damage in glaucoma as transgenic Ucp2 overexpression. To test this hypothesis, we increased IOP in control- and RSG-fed WT mice (**Figure 7A**) and measured RGC loss 30 days following bead injection. There was an 11±2% loss in RGC density in bead-injected eyes of WT control mice ($n = 3$), compared to a 17±2% loss in RSG-fed mice ($n = 4$). The degree of cell loss was generally lesser than for $Ucp2^{KI}$ controls, which can be explained by the more advanced age of these mice (3.8 months), which has been demonstrated to reduce the effectiveness of RGC loss following bead injection (Cone et al., 2010). Regardless, the result of this pilot study on the effects of RSG ran contrary to our expectations and did not decrease RGC death, and in fact appeared to non-significantly increase RGC loss (**Figures 7C,D**).

DISCUSSION

Mild levels of ROS are important signals of mitochondrial damage (Frank et al., 2012) among other physiological signals (Angelova and Abramov, 2016). When ROS production exceeds the capacity for detoxification by antioxidants, they damage cellular components in a variety of pathogenic conditions (Elfawy and Das, 2019). More reduced electron transport chain metabolites (NADH, coenzyme Q_{10}) are better able to form ROS. Inhibitors of electrons transport, such as the Coenzyme Q_{10}-cytochrome C Oxidoreductase (complex III) inhibitor AA, increase the accumulation of reduced electron carriers and consequently drive mitochondrial ROS production (Quinlan et al., 2011). However, ROS production is partially dependent on a high Ψ_m (Korshunov et al., 1997; Miwa et al., 2003), which can be depolarized by either an FCCP- or Ucp2-mediated increase in proton conductance (Nègre-Salvayre et al., 1997). These data were mainly gathered in isolated mitochondria. Tissue mitochondrial quantity is too small in the retina and optic nerve, and with our currently available tools, we cannot determine endogenous RGC and optic nerve head astrocyte-specific relations between ROS and Ψ_m, if such relations exist. However, given identical bioenergetic circumstances most cellular mitochondria should react similarly to agents that alter mitochondrial coupling or electron transport. Similarly, our use of transgenic *Ucp2* overexpression is not under the control of endogenous regulatory factors, which are more likely to differ with cell type and condition.

Given the similarity of mitochondrial respiratory chain function across cell types, we used primary cortical astrocytes to demonstrate the concepts that AA-stimulated increases in ROS production that are attenuated by decreases in Ψ_m (**Figure 1**), and that *Ucp2* decreases ROS production (**Figure 2**). While these data lend support to the association between mitochondrial Ψ_m and ROS as well as the control of ROS by *Ucp2*, the most important evidence for their effect on cell and tissue physiology normally and during glaucoma must be determined *in vivo*.

Mitochondria are damaged in both glaucomatous retinal and optic nerve tissue (Coughlin et al., 2015) as well as in systemic circulation of glaucoma patients (Van Bergen et al., 2015). Mitochondria are a major source of ROS, so mitochondrial dysfunction in glaucoma is a likely source of ROS in the same tissues (Feilchenfeld et al., 2008; Chidlow et al., 2017). As with cultured cells, partial dissipation of tissue mitochondrial Ψ_m may decrease the generation of ROS in glaucoma (**Figure 6**).

Ucp2 expression is in fact altered during different stages of glaucoma, and appears to increase with increasing IOP (**Figure 3**). In pilot samples, however, we note that longer periods (30 days) following bead injection result in a depression of Ucp2 expression to roughly 80% of contralateral controls (data not shown). This is consistent with other studies of Ucp2 expression following a damaging insult, wherein tissue Ucp2 expression peaks 3–5 days after an insult (Rupprecht et al., 2012; Dutra et al., 2018). It is likely that over time in glaucoma, *Ucp2* levels may fall, and this may be correlated with RGC loss (Howell et al., 2011). If increased ganglion cell *Ucp2* expression reflects a physiological response to increased ROS early in glaucoma, artificially increasing Ucp2 may increase the ability of that stress response to increase cell survival. We indeed found an increase in retinal *Ucp2* expression following microbead injection (**Figure 5**). The hypothesis that *Ucp2* improves cell survival following a cellular stressor is also strongly supported by previous studies (Diano et al., 2003; Mattiasson et al., 2003; Andrews et al., 2005; Barnstable et al., 2016), but the novelty of our study is that in rodent models of glaucoma, RGC death is progressive over time (Huang et al., 2018), suggesting that Ucp2 is not exclusively protective during acutely stressful conditions, but also during sub-acute neurodegeneration, decreasing the accumulation of oxidative damage (**Figure 6**) and bead-induced RGC loss.

Ucp2-mediated neuroprotection is dependent on cell type, as we show that greater *Ucp2* levels in *Gfap*-expressing glia do not significantly alter RGC loss or oxidative stress-derive protein carbonyls compared to controls (**Figures 5**, **6**). A larger sample size may benefit these studies and be sufficient to demonstrate a glial-derived neuroprotective effect, supported by a trend toward decreased oxidative stress and RGC loss in $Ucp2^{KI}$; $GFAP\text{-}creER^{T2}$ mice, but overall the data argue for much weaker if any *Ucp2*-mediated neuroprotection from glial cells than from RGCs. This seems to suggest that changes in mitochondrial dynamics within *Gfap*-expressing glia of the retina may not be central for the progression of glaucoma, which is unexpected given the many changes they undergo over the course of the disease (Woldemussie et al., 2004) and the protection they give to RGCs (Kawasaki et al., 2000).

Rosiglitazone is a PPAR-γ-dependent transcriptional activator of *Ucp2* (Medvedev et al., 2001; Chen et al., 2006), and increases retinal *Ucp2* expression (**Figure 7**), but does not seem to promote *Ucp2* mediated neuroprotection in the microbead model of glaucoma. PPAR-γ appears to be expressed with high specificity in müller glia cells of the rodent retina (Zhu et al., 2013), and while the failure of RSG to protect RGCs was initially surprising, it likely increases the transcription of glial *Ucp2*. *Ucp2* overexpression in *Gfap*-expressing glia failed to protect RGCs, so our experiments using RSG-fed and $Ucp2^{KI}$; $GFAP\text{-}creER^{T2}$ mice largely support each other. PPAR-γ agonism with pioglitazone is sufficient to decrease RGC loss following optic nerve crush in rats (Zhu et al., 2013) or retinal ischemia/reperfusion injury in mice (Zhang et al., 2017), suggesting that glial *Ucp2* expression may be protective against more acute retinal insults. This protection may also result from the increase in neural PPAR-γ following optic nerve crush (Zhu et al., 2013), which would allow for agonist-stimulated Ucp2 mRNA expression that is likely subject to multiple endogenous regulatory mechanisms (Donadelli et al., 2014), unlike the *Ucp2* derived from our transgenic mice (Toda et al., 2016). Alternatively, PPAR-γ could theoretically promote multiple counteracting effects that render transcriptional stimulation of Ucp2 unimportant in glaucoma. For example, activation of PPAR-γ promotes fatty acid oxidation (Benton et al., 2008), increasing use of a bioenergetic substrate that may directly

increase ROS generation (St-Pierre et al., 2002) and thus mask a Ucp2-dependent anti-oxidative effect. Regardless, a larger study of *Ucp2* and PPAR-γ in retinal disease that uses multiple models and agonists/antagonists may yield a clearer picture that captures the cell type specific dynamics of these factors, and changes during different paradigms of retinal damage.

Overall, our data suggest that the greatest protection against RGC loss can be provided by stimulating Ucp2 expression in RGCs. Expression of this gene in other cell types may not be harmful, but our results suggest that the choice of therapeutic target should be dictated in part by cell type. The expression and activity of this protein is also tightly regulated, so the future studies on *Ucp2*-mediated neuroprotection should also focus on the factors that manipulate *Ucp2* transcription, translation, and functional activity.

DATA AVAILABILITY

The datasets generated for this study are available on request to the corresponding author.

AUTHOR CONTRIBUTIONS

DH performed the experiments, analyzed them, and wrote the first draft of the manuscript. Both DH and CB conceived of the study topic and design, as well as revised the submitted manuscript.

FUNDING

This work was supported by grants from the NIH (Grant No. NS100508-01A1 from the NINDS) and the Macula Vision Research Foundation, and a Summer Student Fellowship from Fight for Sight (Grant No. FFS-SS-18-046).

ACKNOWLEDGMENTS

We thank Sabrina Diano, Ph.D., for generously donating the Ucp2KOKI$^{fl/fl}$ mice that were the progenitors of mice used in this study. We also thank Evgenya Popova, Ph.D., for her thorough discussions on and critical review of this research.

REFERENCES

Abu-Amero, K. K., Morales, J., and Bosley, T. M. (2006). Mitochondrial abnormalities in patients with primary open-angle glaucoma. *Invest. Ophthalmol. Vis. Sci.* 47, 2533–2541. doi: 10.1167/iovs.05-1639

Andrews, Z. B., Horvath, B., Barnstable, C. J., Elsworth, J., Elseworth, J., Yang, L., et al. (2005). Uncoupling protein-2 is critical for nigral dopamine cell survival in a mouse model of Parkinson's disease. *J. Neurosci.* 25, 184–191. doi: 10.1523/JNEUROSCI.4269-04.2005

Angelova, P. R., and Abramov, A. Y. (2016). Functional role of mitochondrial reactive oxygen species in physiology. *Free Radic. Biol. Med.* 100, 81–85. doi: 10.1016/j.freeradbiomed.2016.06.005

Barnstable, C. J., Reddy, R., Li, H., and Horvath, T. L. (2016). Mitochondrial Uncoupling Protein 2 (UCP2) regulates retinal ganglion cell number and survival. *J. Mol. Neurosci.* 58, 461–469. doi: 10.1007/s12031-016-0728-5

Benton, C. R., Holloway, G. P., Campbell, S. E., Yoshida, Y., Tandon, N. N., Glatz, J. F., et al. (2008). Rosiglitazone increases fatty acid oxidation and fatty acid translocase (FAT/CD36) but not carnitine palmitoyltransferase I in rat muscle mitochondria. *J. Physiol.* 586, 1755–1766. doi: 10.1113/jphysiol.2007.146563

Boland, M. V., and Quigley, H. A. (2007). Risk factors and open-angle glaucoma: classification and application. *J. Glaucoma* 16, 406–418. doi: 10.1097/IJG.0b013e31806540a1

Carter-Dawson, L., Shen, F., Harwerth, R. S., Smith, E. L., Crawford, M. L., and Chuang, A. (1998). Glutamine immunoreactivity in Müller cells of monkey eyes with experimental glaucoma. *Exp. Eye Res.* 66, 537–545. doi: 10.1006/exer.1997.0447

Chen, S. D., Wu, H. Y., Yang, D. I., Lee, S. Y., Shaw, F. Z., Lin, T. K., et al. (2006). Effects of rosiglitazone on global ischemia-induced hippocampal injury and expression of mitochondrial uncoupling protein 2. *Biochem. Biophys. Res. Commun.* 351, 198–203. doi: 10.1016/j.bbrc.2006.10.017

Chidlow, G., Wood, J. P. M., and Casson, R. J. (2017). Investigations into hypoxia and oxidative stress at the optic nerve head in a rat model of glaucoma. *Front. Neurosci.* 11:478. doi: 10.3389/fnins.2017.00478

Cone, F. E., Gelman, S. E., Son, J. L., Pease, M. E., and Quigley, H. A. (2010). Differential susceptibility to experimental glaucoma among 3 mouse strains using bead and viscoelastic injection. *Exp. Eye Res.* 91, 415–424. doi: 10.1016/j.exer.2010.06.018

Cone, F. E., Steinhart, M. R., Oglesby, E. N., Kalesnykas, G., Pease, M. E., and Quigley, H. A. (2012). The effects of anesthesia, mouse strain and age on intraocular pressure and an improved murine model of experimental glaucoma. *Exp. Eye Res.* 99, 27–35. doi: 10.1016/j.exer.2012.04.006

Coughlin, L., Morrison, R. S., Horner, P. J., and Inman, D. M. (2015). Mitochondrial morphology differences and mitophagy deficit in murine glaucomatous optic nerve. *Invest. Ophthalmol. Vis. Sci.* 56, 1437–1446. doi: 10.1167/iovs.14-16126

Diano, S., Matthews, R. T., Patrylo, P., Yang, L., Beal, M. F., Barnstable, C. J., et al. (2003). Uncoupling protein 2 prevents neuronal death including that occurring during seizures: a mechanism for preconditioning. *Endocrinology* 144, 5014–5021. doi: 10.1210/en.2003-0667

Donadelli, M., Dando, I., Fiorini, C., and Palmieri, M. (2014). UCP2, a mitochondrial protein regulated at multiple levels. *Cell. Mol. Life Sci.* 71, 1171–1190. doi: 10.1007/s00018-013-1407-0

Dutra, M. R. H., Feliciano, R. D. S., Jacinto, K. R., Gouveia, T. L. F., Brigidio, E., Serra, A. J., et al. (2018). Protective role of UCP2 in oxidative stress and apoptosis during the silent phase of an experimental model of epilepsy induced by pilocarpine. *Oxid. Med. Cell. Longev.* 2018:6736721. doi: 10.1155/2018/6736721

Echtay, K. S., Winkler, E., Frischmuth, K., and Klingenberg, M. (2001). Uncoupling proteins 2 and 3 are highly active H(+) transporters and highly nucleotide sensitive when activated by coenzyme Q (ubiquinone). *Proc. Natl. Acad. Sci. U.S.A.* 98, 1416–1421. doi: 10.1073/pnas.98.4.1416

Elfawy, H. A., and Das, B. (2019). Crosstalk between mitochondrial dysfunction, oxidative stress, and age related neurodegenerative disease: etiologies and therapeutic strategies. *Life Sci.* 218, 165–184. doi: 10.1016/j.lfs.2018.12.029

Feilchenfeld, Z., Yücel, Y. H., and Gupta, N. (2008). Oxidative injury to blood vessels and glia of the pre-laminar optic nerve head in human glaucoma. *Exp. Eye Res.* 87, 409–414. doi: 10.1016/j.exer.2008.07.011

Fleury, C., Neverova, M., Collins, S., Raimbault, S., Champigny, O., Levi-Meyrueis, C., et al. (1997). Uncoupling protein-2: a novel gene linked to obesity and hyperinsulinemia. *Nat. Genet.* 15, 269–272. doi: 10.1038/ng0397-269

Frank, M., Duvezin-Caubet, S., Koob, S., Occhipinti, A., Jagasia, R., Petcherski, A., et al. (2012). Mitophagy is triggered by mild oxidative stress in a mitochondrial fission dependent manner. *Biochim. Biophys. Acta* 1823, 2297–2310. doi: 10.1016/j.bbamcr.2012.08.007

Ganat, Y. M., Silbereis, J., Cave, C., Ngu, H., Anderson, G. M., Ohkubo, Y., et al. (2006). Early postnatal astroglial cells produce multilineage precursors and neural stem cells *in vivo*. *J. Neurosci.* 26, 8609–8621.

Howell, G. R., Macalinao, D. G., Sousa, G. L., Walden, M., Soto, I., Kneeland, S. C., et al. (2011). Molecular clustering identifies complement and endothelin

induction as early events in a mouse model of glaucoma. *J. Clin. Invest.* 121, 1429–1444. doi: 10.1172/JCI44646

Howell, G. R., MacNicoll, K. H., Braine, C. E., Soto, I., Macalinao, D. G., Sousa, G. L., et al. (2014). Combinatorial targeting of early pathways profoundly inhibits neurodegeneration in a mouse model of glaucoma. *Neurobiol. Dis.* 71, 44–52. doi: 10.1016/j.nbd.2014.07.016

Huang, W., Hu, F., Wang, M., Gao, F., Xu, P., Xing, C., et al. (2018). Comparative analysis of retinal ganglion cell damage in three glaucomatous rat models. *Exp. Eye Res.* 172, 112–122. doi: 10.1016/j.exer.2018.03.019

Ito, Y. A., and Di Polo, A. (2017). Mitochondrial dynamics, transport, and quality control: a bottleneck for retinal ganglion cell viability in optic neuropathies. *Mitochondrion* 36, 186–192. doi: 10.1016/j.mito.2017.08.014

Izzotti, A., Saccà, S. C., Cartiglia, C., and De Flora, S. (2003). Oxidative deoxyribonucleic acid damage in the eyes of glaucoma patients. *Am. J. Med.* 114, 638–646. doi: 10.1016/S0002-9343(03)00114-1

Kawasaki, A., Otori, Y., and Barnstable, C. J. (2000). Müller cell protection of rat retinal ganglion cells from glutamate and nitric oxide neurotoxicity. *Invest. Ophthalmol. Vis. Sci.* 41, 3444–3450.

Klingenberg, M., and Rottenberg, H. (1977). Relation between the gradient of the ATP/ADP ratio and the membrane potential across the mitochondrial membrane. *Eur. J. Biochem.* 73, 125–130. doi: 10.1111/j.1432-1033.1977.tb11298.x

Korshunov, S. S., Skulachev, V. P., and Starkov, A. A. (1997). High protonic potential actuates a mechanism of production of reactive oxygen species in mitochondria. *FEBS Lett.* 416, 15–18. doi: 10.1016/S0014-5793(97)01159-9

Lapp, D. W., Zhang, S. S., and Barnstable, C. J. (2014). Stat3 mediates LIF-induced protection of astrocytes against toxic ROS by upregulating the UPC2 mRNA pool. *Glia* 62, 159–170. doi: 10.1002/glia.22594

Leske, M. C., Heijl, A., Hyman, L., Bengtsson, B., and Komaroff, E. (2004). Factors for progression and glaucoma treatment: the early manifest glaucoma trial. *Curr. Opin. Ophthalmol.* 15, 102–106. doi: 10.1097/00055735-200404000-00008

Malone, P. E., and Hernandez, M. R. (2007). 4-Hydroxynonenal, a product of oxidative stress, leads to an antioxidant response in optic nerve head astrocytes. *Exp. Eye Res.* 84, 444–454. doi: 10.1016/j.exer.2006.10.020

Mattiasson, G., Shamloo, M., Gido, G., Mathi, K., Tomasevic, G., Yi, S., et al. (2003). Uncoupling protein-2 prevents neuronal death and diminishes brain dysfunction after stroke and brain trauma. *Nat. Med.* 9, 1062–1068. doi: 10.1038/nm903

Medvedev, A. V., Snedden, S. K., Raimbault, S., Ricquier, D., and Collins, S. (2001). Transcriptional regulation of the mouse uncoupling protein-2 gene. Double E-box motif is required for peroxisome proliferator-activated receptor-gamma-dependent activation. *J. Biol. Chem.* 276, 10817–10823. doi: 10.1074/jbc.M010587200

Miwa, S., St-Pierre, J., Partridge, L., and Brand, M. D. (2003). Superoxide and hydrogen peroxide production by Drosophila mitochondria. *Free Radic. Biol. Med.* 35, 938–948. doi: 10.1016/S0891-5849(03)00464-7

Munemasa, Y., Ahn, J. H., Kwong, J. M., Caprioli, J., and Piri, N. (2009). Redox proteins thioredoxin 1 and thioredoxin 2 support retinal ganglion cell survival in experimental glaucoma. *Gene Ther.* 16, 17–25. doi: 10.1038/gt.2008.126

Nègre-Salvayre, A., Hirtz, C., Carrera, G., Cazenave, R., Troly, M., Salvayre, R., et al. (1997). A role for uncoupling protein-2 as a regulator of mitochondrial hydrogen peroxide generation. *FASEB J.* 11, 809–815. doi: 10.1096/fasebj.11.10.9271366

Pinzon-Guzman, C., Zhang, S. S., and Barnstable, C. J. (2011). Specific protein kinase C isoforms are required for rod photoreceptor differentiation. *J. Neurosci.* 31, 18606–18617. doi: 10.1523/JNEUROSCI.2578-11.2011

Piotrowska-Nowak, A., Kosior-Jarecka, E., Schab, A., Wrobel-Dudzinska, D., Bartnik, E., Zarnowski, T., et al. (2018). Investigation of whole mitochondrial genome variation in normal tension glaucoma. *Exp. Eye Res.* 178, 186–197. doi: 10.1016/j.exer.2018.10.004

Quigley, H. A. (2011). Glaucoma. *Lancet* 377, 1367–1377. doi: 10.1016/S0140-6736(10)61423-7

Quinlan, C. L., Gerencser, A. A., Treberg, J. R., and Brand, M. D. (2011). The mechanism of superoxide production by the antimycin-inhibited mitochondrial Q-cycle. *J. Biol. Chem.* 286, 31361–31372. doi: 10.1074/jbc.M111.267898

Ramdas, W. D., Schouten, J. S. A. G., and Webers, C. A. B. (2018). The effect of vitamins on glaucoma: a systematic review and meta-analysis. *Nutrients* 10:E359. doi: 10.3390/nu10030359

Resnikoff, S., and Keys, T. U. (2012). Future trends in global blindness. *Indian J. Ophthalmol.* 60, 387–395. doi: 10.4103/0301-4738.100532

Rodriguez, A. R., de Sevilla Müller, L. P., and Brecha, N. C. (2014). The RNA binding protein RBPMS is a selective marker of ganglion cells in the mammalian retina. *J. Comp. Neurol.* 522, 1411–1443. doi: 10.1002/cne.23521

Rupprecht, A., Bräuer, A. U., Smorodchenko, A., Goyn, J., Hilse, K. E., Shabalina, I. G., et al. (2012). Quantification of uncoupling protein 2 reveals its main expression in immune cells and selective up-regulation during T-cell proliferation. *PLoS One* 7:e41406. doi: 10.1371/journal.pone.0041406

Saccà, S. C., and Izzotti, A. (2008). Oxidative stress and glaucoma: injury in the anterior segment of the eye. *Prog. Brain Res.* 173, 385–407. doi: 10.1016/S0079-6123(08)01127-8

Sarafian, T. A., Montes, C., Imura, T., Qi, J., Coppola, G., Geschwind, D. H., et al. (2010). Disruption of astrocyte STAT3 signaling decreases mitochondrial function and increases oxidative stress in vitro. *PLoS One* 5:e9532. doi: 10.1371/journal.pone.0009532

St-Pierre, J., Buckingham, J. A., Roebuck, S. J., and Brand, M. D. (2002). Topology of superoxide production from different sites in the mitochondrial electron transport chain. *J. Biol. Chem.* 277, 44784–44790. doi: 10.1074/jbc.M207217200

Takihara, Y., Inatani, M., Eto, K., Inoue, T., Kreymerman, A., Miyake, S., et al. (2015). In vivo imaging of axonal transport of mitochondria in the diseased and aged mammalian CNS. *Proc. Natl. Acad. Sci. U.S.A.* 112, 10515–10520. doi: 10.1073/pnas.1509879112

Tezel, G., Yang, X., and Cai, J. (2005). Proteomic identification of oxidatively modified retinal proteins in a chronic pressure-induced rat model of glaucoma. *Invest. Ophthalmol. Vis. Sci.* 46, 3177–3187. doi: 10.1167/iovs.05-0208

Toda, C., Kim, J. D., Impellizzeri, D., Cuzzocrea, S., Liu, Z. W., and Diano, S. (2016). UCP2 regulates mitochondrial fission and ventromedial nucleus control of glucose responsiveness. *Cell* 164, 872–883. doi: 10.1016/j.cell.2016.02.010

Van Bergen, N. J., Crowston, J. G., Craig, J. E., Burdon, K. P., Kearns, L. S., Sharma, S., et al. (2015). Measurement of systemic mitochondrial function in advanced primary open-angle glaucoma and leber hereditary optic neuropathy. *PLoS One* 10:e0140919. doi: 10.1371/journal.pone.0140919

Varela, H. J., and Hernandez, M. R. (1997). Astrocyte responses in human optic nerve head with primary open-angle glaucoma. *J. Glaucoma* 6, 303–313. doi: 10.1097/00061198-199710000-00007

Williams, P. A., Harder, J. M., Foxworth, N. E., Cochran, K. E., Philip, V. M., Porciatti, V., et al. (2017). Vitamin B3 modulates mitochondrial vulnerability and prevents glaucoma in aged mice. *Science* 355, 756–760. doi: 10.1126/science.aal0092

Woldemussie, E., Wijono, M., and Ruiz, G. (2004). Müller cell response to laser-induced increase in intraocular pressure in rats. *Glia* 47, 109–119. doi: 10.1002/glia.20000

Young, P., Qiu, L., Wang, D., Zhao, S., Gross, J., and Feng, G. (2008). Single-neuron labeling with inducible Cre-mediated knockout in transgenic mice. *Nat. Neurosci.* 11, 721–728. doi: 10.1038/nn.2118

Zhang, Y., Riesterer, C., Ayrall, A. M., Sablitzky, F., Littlewood, T. D., and Reth, M. (1996). Inducible site-directed recombination in mouse embryonic stem cells. *Nucleic Acids Res.* 24, 543–548. doi: 10.1093/nar/24.4.543

Zhang, Y. L., Wang, R. B., Li, W. Y., Xia, F. Z., and Liu, L. (2017). Pioglitazone ameliorates retinal ischemia/reperfusion injury. *Int. J. Ophthalmol.* 10, 1812–1818. doi: 10.18240/ijo.2017.12.04

Zhu, J., Zhang, J., Ji, M., Gu, H., Xu, Y., Chen, C., et al. (2013). The role of peroxisome proliferator-activated receptor and effects of its agonist, pioglitazone, on a rat model of optic nerve crush: PPARγ in retinal neuroprotection. *PLoS One* 8:e68935. doi: 10.1371/journal.pone.0068935

Conflict of Interest Statement: The authors declare that the research was conducted in the absence of any commercial or financial relationships that could be construed as a potential conflict of interest.